

Fracture of Ferritic Steels; the effects of the Ductile Brittle Transition on Carbides within the Plastic Zone

M. D. Coates, S. G. Roberts

Department of Materials Science, University of Oxford.

Abstract

Ferritic steels undergo a ductile to brittle transition (DBT) with decreasing temperature. The transition temperature may typically be 50°C to 100°C wide, centred around -50°C to 0°C. As temperature falls within this range, the fracture toughness drops from more than 100MPam^{1/2} to less than 40 MPam^{1/2} and the fracture mode changes from rupture to cleavage. The controlling process leading to cleavage is the propagation of a crack from a fractured brittle carbide particle. This work investigates the effects of cracked carbides in the plastic zone ahead of a loaded crack. A heat treatment of 40 hours at 650°C has been applied to A533B steel to produce a homogenous spheroidised microstructure. Carbides have been investigated using TEM. The work has focused on producing experimental data of cleavage fracture around the lower shelf of the DBT. This paper shows the variation of yield stress with temperature and using the 'master curve' approach, the variation in fracture toughness with temperature. It will then be shown that a modelling approach to predicting cleavage behaviour can be coupled with microstructural parameters, and not simply solved empirically.

Keywords

Ductile, Brittle, Transition, Carbides, Fracture, Plastic Zone, Cleavage.

Introduction

Hirsch, Roberts et al at Oxford, over the past ten years, have been very successful in predicting the fracture behaviour of single crystals such as pure silicon, germanium, alumina and molybdenum [1,2,3]. Most recently the models have been extended to materials where the dislocation velocity law contains a significant friction stress, below which the dislocations will not move (i.e. the kind of behaviour expected in steels). It has then been found that the predicted plastic zone sizes and configurations, the crack opening displacement and the crack tip stress fields, follow very closely the 'classic' earlier models based on dislocations [4,5].

This paper presents experimental work aimed at providing experimental data on a material with a model ferrite/carbide microstructure, to correlate modelling of this type.

Experimental Methods

The steel chosen for the investigation was an A533-B pressure vessel steel produced by Ross and Cathedral, Sheffield. It was produced from electrolytic vacuum degassed iron with no single impurity greater than 100ppm. All alloying elements were pure. The composition is given in table 1.

TABLE 1.
Composition of A533-B pressure vessel steel in wt.%

Carbon	Manganese	Molybdenum	Nickel	Silicon	Phosphorus	Sulphur	Copper
0.24	1.37	0.52	0.5	0.23	0.003	0.005	<0.01

The steel was heat-treated 40 hours at 650°C with the aim of producing a microstructure of spherical brittle carbides in a relatively clean ferrite matrix. Fracture specimen dimensions are shown in figure 1.

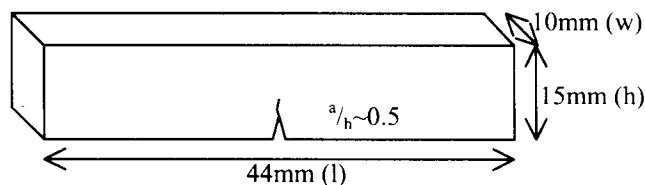


Figure 1. Specimen dimensions.

The total crack length (a) is between 5mm and 6mm leading to an a/h ratio of between 0.46 and 0.53. The crack was introduced into the specimen by fatigue in three point bending. Initial fatiguing was at 10Hz for 50,000 cycles with a surface stress of around 400MPa. Once the crack was initiated the surface stress was reduced to 350MPa for a further 50,000 cycles before being reduced to 250MPa until the a/h ratio reached the desired value. All fatiguing was carried out at room temperature. Samples were then fractured in four point bend under displacement control at 0.25mm/min, over a range of temperatures from -192°C to +120°C. The cold tests used liquid nitrogen; temperatures above ambient were achieved using nitrogen passed through heating coils in a furnace and the use of a high-powered halogen heating lamp. Temperature control was enabled through type K thermocouples attached to the specimen and was stable within $\pm 2^\circ\text{C}$.

At low temperatures fracture loads were measured at the point of catastrophic failure (coincident with initiation). At temperatures above -30°C, no such unstable fracture occurred and the fracture loads were now measured at initiation. The point of initiation could be identified from inflections in the load-displacement curves. The mode of initiation at each temperature was determined by completely fracturing the specimens in liquid nitrogen and examining the fracture surfaces both optically and in the scanning electron microscope.

Uniaxial tensile properties were determined over a similar temperature range by testing modified Hounsfield specimens, figure 2, machined from the fracture specimens. The tests were displacement controlled with an operating actuator speed of 0.5mm/min (strain rate of $6.41 \times 10^{-4} \text{s}^{-1}$). Yield stress was measured at the onset of plastic deformation determined by examining the force-displacement data.

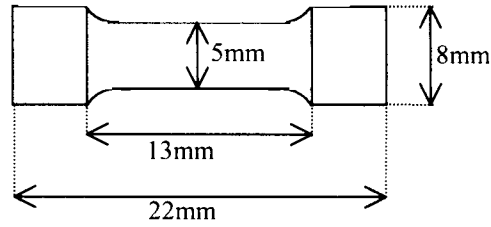


Figure 2. Dimensions of the tensile test specimen.
Radius of curvature of the inner-outer gauge is 1mm

Two sets of fracture tests were completed. Set A was used to gain an overview of the toughness temperature curve. The samples were fatigued at a constant load until the desired crack length was obtained. The crack length was also shorter so that $a/h \sim 0.25-0.35$. The samples were also quenched from 650°C to room temperature. In set B the fatigue process was modified to that set out above and quenching was replaced by a slow cool over 12 hours. These specimens were used to study variability of behaviour at two temperatures.

Experimental Results

Many of the test specimens exhibited significant plastic flow before fracture, so fracture data were analysed in terms of the J-integral. ASTM E1921-98 [6] was used for validation J_C analysis. Figure 3 shows fracture toughness, K_{JC} , versus temperature for all specimens tested.

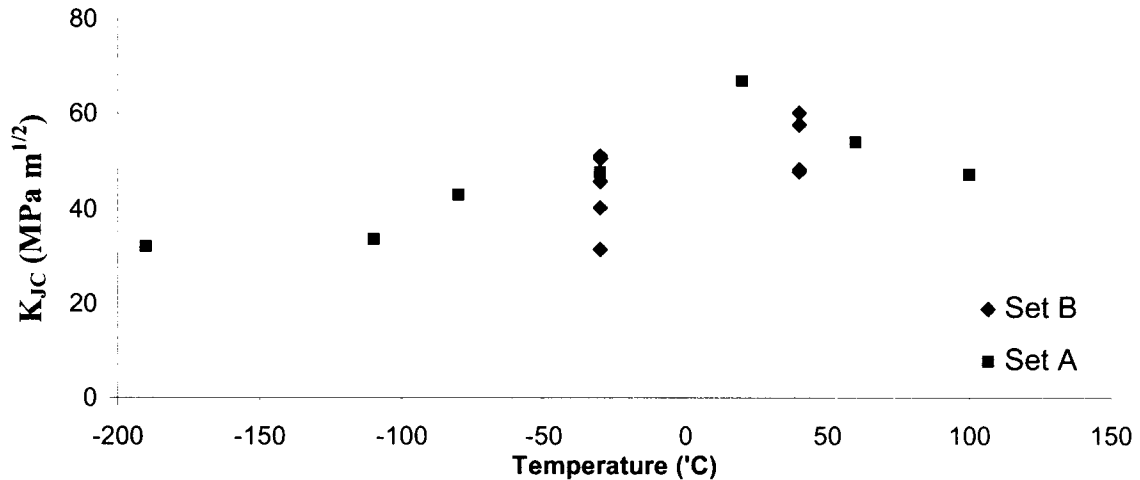


Figure 3. K_{JC} as a function of temperature.

The test results were then analysed using the ‘master curve’ approach of Wallin et al [7]. In the master curve concept, a universal form of temperature dependence for cleavage fracture toughness is assumed (equation 6), if data are scaled to a material-dependent reference temperature T_0 .

$$K_0 = 31 + 77 \cdot \exp\{0.019 \cdot (T - T_0)\} \quad (6)$$

$$\sum_{i=1}^n \frac{\exp\{0.019 \cdot [T_i - T_0]\}}{11 + 77 \cdot \exp\{0.019 \cdot [T_i - T_0]\}} - \sum_{i=1}^n \frac{(K_{iC} - 20)^4 \cdot \exp\{0.019 \cdot [T_i - T_0]\}}{(11 + 77 \cdot \exp\{0.019 \cdot [T_i - T_0]\})^5} = 0 \quad (7)$$

Two methods of estimating the master curve transition temperature T_0 were used. The first method used both set A and set B data. T_0 was calculated from the size adjusted K_{JC} data using a multi-temperature randomly censored maximum likelihood expression given in equation 7 (figure 4). The

second method used data determined to be on the lower shelf (by examining the Force-Displacement curves and where in doubt, the examination of fracture surfaces) and followed the same calculation. Results are shown in figure 5. Results that did not meet the ASTM validity requirements were not included in either master curve calculation.

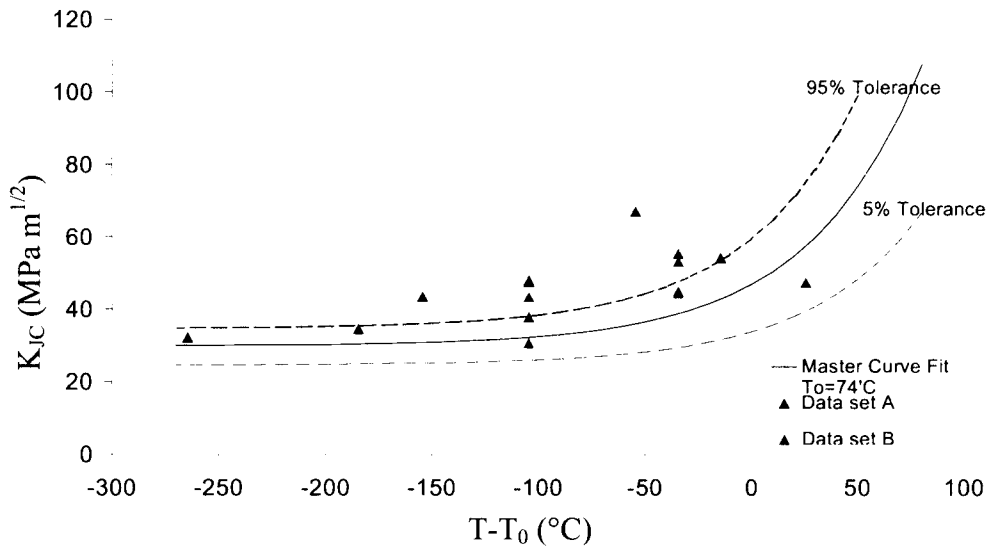


Figure 4. The master curve $T_0=74^\circ\text{C}$ using equation 7, with all data present.

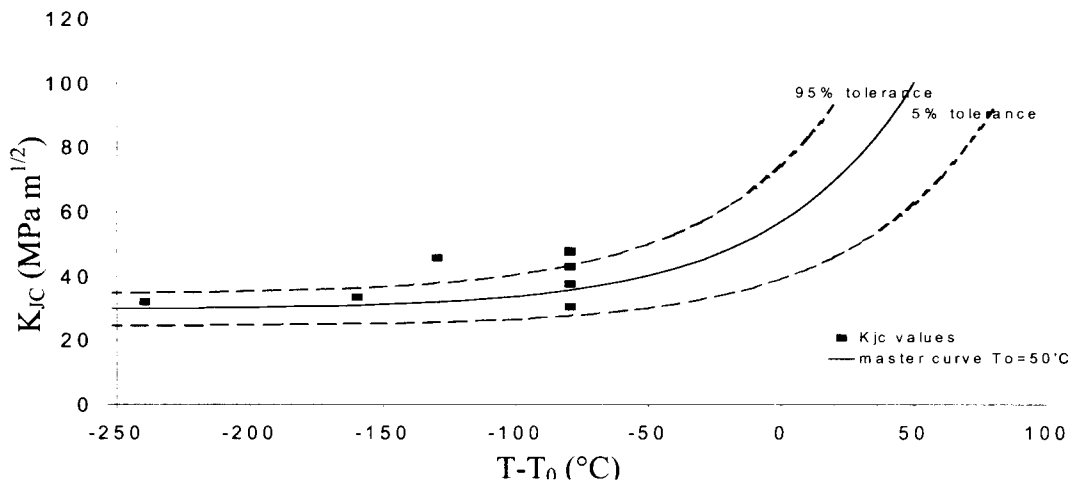


Figure 5. The master curve calculated using cleavage data.

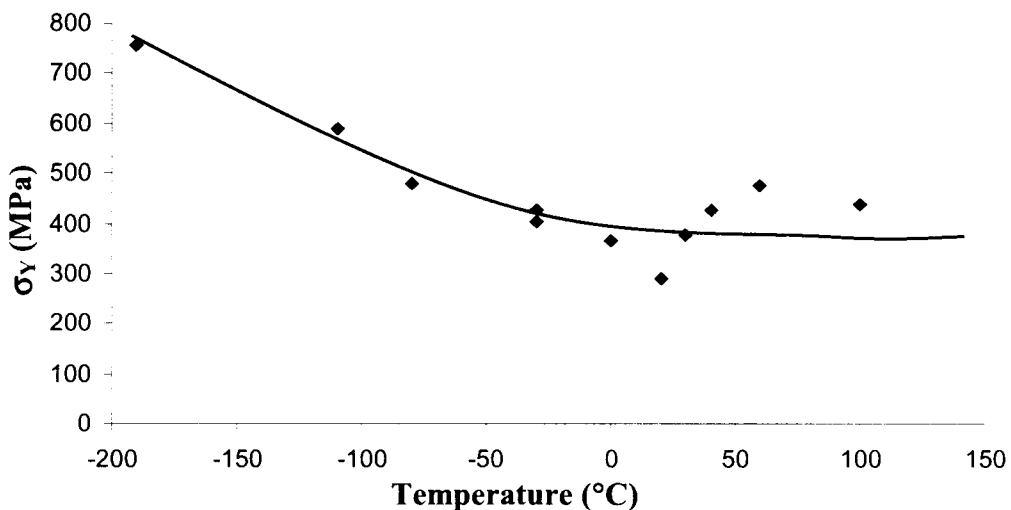


Figure 6. Variation of yield stress with temperature.

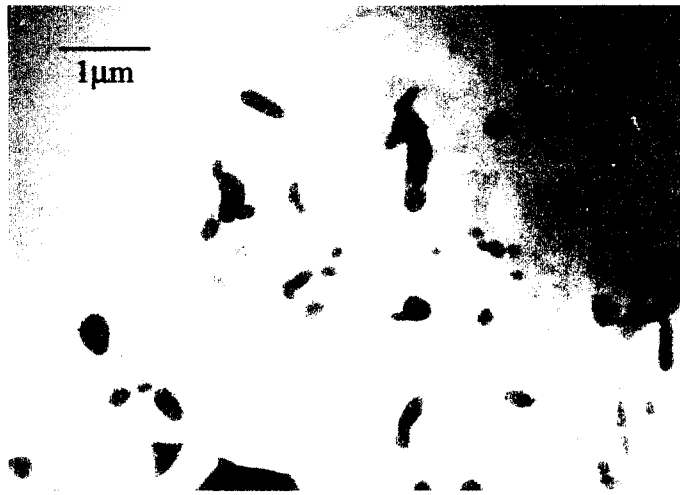


Figure 7. A typical microstructure for a heat-treatment of 40 hours at 650°C.

Image analysis of TEM micrographs was used to determine carbide sizes and spacing. The size was taken as an area measurement and then converted to an equivalent radius. The spacing was taken as the nearest neighbour distance. Carbide size was $0.8\mu\text{m} \pm 0.2\mu\text{m}$, and inter particle spacing $0.5\mu\text{m} \pm 0.15\mu\text{m}$.

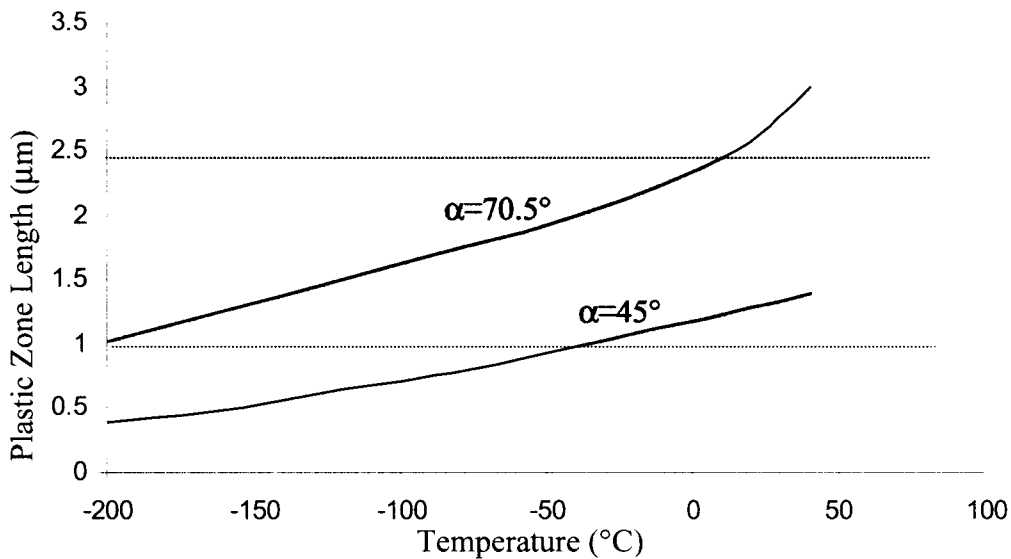


Figure 7. Relationship between the modelled array lengths. α is the slip plane angle and the shading shows the range the transition temperature falls.

These data can be used to link the fracture data presented here and results from dislocation-level simulations of crack tip plastic zones. Figure 7 shows the produced length of crack tip plastic zone size modelled with cracked particles of $0.8\mu\text{m}$ diameter, as a function of temperature. The modelling simulates the plastic zone as a single slip plane on which dislocations glide away from the crack under the influence of a local stress (the slip plane is at an angle α to the crack plane). Dislocations are assumed to halt at a temperature-dependent friction stress (the yield stress data in figure 6 was used here). Dislocation array/plastic zone length shown in figure 7 is thus achieved just before fracture would propagate from the cracked carbide into the matrix, triggering cleavage of the specimen.

Conclusion

The microstructure of a steel has been modified to produce a simplified microstructure of spherical carbides in a ferrite matrix, better suited to modelling crack tip stress fields around carbides. The changes in microstructure have led to a horizontal shift and flattening of the apparent DBT, with low upper-shelf values for K_{IC} . The J-integral method and the master curve method have been used to identify the transition temperature, T_0 . T_0 varies depending on the mode of fracture but this is likely to arise out of a certain invalidity for K_{IC} values above room temperature.

Modelling of plastic zones and crack tips carried out to date correlates well with the experimental data in that, at the transition temperature, the predicted plastic zone length for carbides of the size seen here is roughly equal to its inter-particle spacing. Further work is in progress to investigate this more completely.

Acknowledgements

This work was supported by the Engineering and Physical Sciences Research Council, UK, under grant number M05188, in collaboration with AEA Technology and the Health and Safety Executive.

References

1. Samuels, J. and Roberts, S.G. (1989) The brittle-ductile transition in silicon. I. experiments, *Proc. R. Soc. Lond. A* **421**, 1-23.
2. Serbena, F.C. and Roberts, S.G. (1994) The brittle ductile transition in germanium, *Acta Metall. Mater.* **42**, 2505-2510
3. Roberts, S.G., Hirsch, P.B., Booth, A.S., Ellis, M. and Serbena, F.C. (1993) Dislocations, cracks and brittleness in single crystals, *Physica Scripta*, **T49**, 420-426.
4. Roberts, S.G. in *Computer Simulation in Materials Science-nano/meso/macrosopic Space and Time Scales*, edited by H.O. Kirchner *et al.* (NATO ASI Series, Series E (Applied Sciences), **308**, Kluwer, Dordrecht, 1996), 409-433.
5. Noronha, S.J., Roberts, S.G. and Wilkinson, A.J. (1999) A multiple slip plane model for crack-tip plasticity. Presented at the MRS Fall 1999 meeting, Boston. Unpublished work.
6. ASTM Standard E1921-98 "Standard test method for determination of reference temperature, T_0 , for ferritic steels in the transition range" pub ASTM vol 03.01 1998.
7. Wallin, K. (1998) Master curve analysis of ductile to brittle transition region fracture toughness round robin data. The "EURO" fracture toughness curve. VTT Pulications. Finland.